Reference 87

# Laser tweezer controlled solid immersion lens for high resolution imaging in microfluidic and biological samples

**Aaron L. Birkbeck[*], Sanja Zlatanovic, Mihrimah Ozkan[†] and Sadik C. Esener**

University of California, San Diego
9500 Gilman Drive, MC 0408
La Jolla, CA 93093-0408

[†] Department of Electrical Engineering /
Chemical and Environmental Engineering
University of California, Riverside
A241 Bourns Hall
Riverside, CA 92521

## ABSTRACT

A novel technique is presented which integrates the capacity of a laser tweezer to optically trap and manipulate objects in three-dimensions with the resolution-enhanced imaging capabilities of a solid immersion lens (SIL). Up to now, solid immersion lens imaging systems have relied upon cantilever-mounted SILs that are difficult to integrate into microfluidic systems and require an extra alignment step with external optics. As an alternative to the current state-of-art, we introduce a device that consists of a free-floating SIL and a laser optical tweezer. In our design, the optical tweezer, created by focusing a laser beam through high numerical aperture microscope objective, acts in a two-fold manner: both as a trapping beam for the positioning and alignment of the SIL and as an near-field scanning beam to image the sample through the SIL. Combining the alignment, positioning, and imaging functions into a single device allows for the direct integration of a high resolution imaging system into microfluidic and biological environments.

**Keywords:** solid immersion lens (SIL), laser tweezer, near-field solid immersion microscopy, microfluidics

## 1. INTRODUCTION

Throughout the past decade there has been tremendous growth in the areas of Bio-MEMS and microfluidic systems using ideas and technologies borrowed from the semiconductor industry. One of the end results of these burgeoning biological fields is an increase in the capability to analyze and manipulate smaller and smaller objects down to the nanometer level of single DNA and protein strands. Since the size of the objects currently under investigation tend to be smaller than the wavelength of visible light, standard microscopy and imaging practices are becoming obsolete. In microscopy, the spot size, which determines the minimum resolvable feature size, is diffraction limited and can be approximated by $\lambda/2NA$, where λ is the free space wavelength and $NA$ is the numerical aperture of the microscope objective. In order to maintain a reasonable working distance, a microscope objective's numerical aperture has an upper limit set by the index of refraction of the medium in which it is imaging, resulting in minimum spot sizes of λ/2 for standard objectives and λ/3 for oil immersion microscope objectives.[1, 2]

In 1990, Gordon S. Kino introduced the idea of the solid immersion lens (SIL)[3, 4] where a high index of refraction hemispherical or superspherical lens is introduced between the microscope objective and the sample yielding an effectively reduced spot size when imaging in the near-field of the SIL. Utilizing the SIL in such an imaging system

[*] alb@ieee.org; phone 1 858 822-4158; fax 1 858 534-1225; soliton.ucsd.edu

# Report Documentation Page

*Form Approved*
*OMB No. 0704-0188*



| 1. REPORT DATE | 2. REPORT TYPE | 3. DATES COVERED |
|---|---|---|
| **01 JUN 2005** | **N/A** | **-** |

| 4. TITLE AND SUBTITLE | 5a. CONTRACT NUMBER |
|---|---|
| **Laser tweezer controlled solid immersion lens for high resolution imaging in microfluidic and biological samples** | 5b. GRANT NUMBER |
| | 5c. PROGRAM ELEMENT NUMBER |
| 6. AUTHOR(S) | 5d. PROJECT NUMBER |
| | 5e. TASK NUMBER |
| | 5f. WORK UNIT NUMBER |
| 7. PERFORMING ORGANIZATION NAME(S) AND ADDRESS(ES) **University of California, San Diego 9500 Gilman Drive, MC 0408 La Jolla, CA 93093-0408** | 8. PERFORMING ORGANIZATION REPORT NUMBER |
| 9. SPONSORING/MONITORING AGENCY NAME(S) AND ADDRESS(ES) | 10. SPONSOR/MONITOR'S ACRONYM(S) |
| | 11. SPONSOR/MONITOR'S REPORT NUMBER(S) |

12. DISTRIBUTION/AVAILABILITY STATEMENT
**Approved for public release, distribution unlimited**

13. SUPPLEMENTARY NOTES
**See also ADM001923.**

14. ABSTRACT

15. SUBJECT TERMS

| 16. SECURITY CLASSIFICATION OF: | | | 17. LIMITATION OF ABSTRACT | 18. NUMBER OF PAGES | 19a. NAME OF RESPONSIBLE PERSON |
|---|---|---|---|---|---|
| a. REPORT | b. ABSTRACT | c. THIS PAGE | | | |
| **unclassified** | **unclassified** | **unclassified** | **UU** | **8** | |

allows for a relaxation in the numerical aperture of the microscope objective and a longer more manageable working distance between the microscope objective and the sample. Since the time of its introduction, the solid immersion lens has been mainly utilized in the field of near-field magneto-optical data storage.[5, 6] This method of solid immersion microscopy relies on a SIL that is mounted on a cantilever and mechanically actuated to maintain the very narrow air gap between the SIL and the sample needed to maximize the resolution of the system.

In order to adapt the solid immersion microscope for use in microfluidics, it is necessary to transition away from the cantilever-mounted SIL since its mechanics and size are not easily integrated into microfluidic systems. To realistically make this conversion, it will be necessary to decrease the size of the SIL from hundreds of microns to microns and provide an alternate method of manipulating the SIL in the microfluidic environment. In this paper we propose the use of a laser optical tweezer in combination with a newly fabricated polymer solid immersion lens as a means of providing high resolution in situ imaging of nanoscale biological entities. In the first part of the paper we will explain the method of fabrication and characterization of the polymer SILs followed by a discussion of the early experiments that we have performed that will make it possible to achieve a microfluidic solid immersion microscope.

## 2. THEORY

### 2.1 Solid Immersion Lens Theory

The SIL is a truncated spherical lens which serves to increase the effective numerical aperture of the optical system by a maximum of $n$ for a hemispherical lens and $n^2$ for a superspherical or Weierstrass lens, where $n$ is the refractive index of the lens material.[3, 5, 7] For both types of lenses, aberration free focusing occurs at the base of the lens and a reduction in the spot size is achieved by a reduction in the wavelength inside the SIL due to the high index of the material and an increase in the incident angle θ, defined as the angle from the most extreme ray to the optical axis, due to the refraction of the rays at the SIL's spherical surface. Due to the high refractive index of the SIL and the large angles of the incident rays, total internal reflection occurs at the base of the SIL and thus the spot size reduction only occurs within the SIL and can only be utilized by placing the sample within the SIL's evanescent decay length or the near field of the SIL.

Currently the bulk of our work is focused on the characteristics of the Weierstrass SIL. This lens is formed by removing the cap or crown of a spherical lens whose thickness is determined by $r\left(1-1/n\right)$, where r is the radius of the sphere. The height or thickness of the truncated sphere can then be represented by $r\left(1+1/n\right)$ and a focused spot will appear at the base of the lens when the incident rays are focused to a distance $nr$ past the center of the SIL. The ratio of the distances $nr$ and $r/n$ leads to a magnification factor of $n^2$ that is independent of the radius of curvature of the lens and acts to increase the effective numerical aperture of the SIL. However, the Weierstrass SIL must still satisfy Abbe's sine condition[8] and therefore, the maximum achievable NA cannot exceed the index of refraction of the SIL[9].

One of the key issues in the fabrication of solid immersion lenses is the spherical aberrations that arise due to errors in the thickness or radius of curvature of the lens. As the size of the SIL decreases, the effects of this spherical aberration become less significant and the allowable tolerances in the thickness of the SIL turn out to be relatively large. The allowable tolerance Δz for a particular wave aberration $\Phi$, where $r$ is the radius of the SIL, $n$ is its refractive index, and $\sin\theta$ is the NA of the objective lens can be calculated with the equation: [10]

$$\Delta z = \sqrt{\frac{8r\Phi}{n\left(n-1\right)\sin^4\theta}} \qquad \textbf{(1)}$$

For a SIL of radius r = 10 μm and index of refraction of n = 1.6, a laser with wavelength λ = 488 nm focused through a microscope objective with a NA = 0.9, and choosing a wave aberration[10] of $\Phi = \lambda/4$ yields a thickness tolerance Δz approximately equal to 3.9 μm. Obviously this tolerance is easily achievable considering that it is equivalent to 39% of the SIL radius.

### 2.2 Laser Tweezer Theory

For objects in the size range of interest of this paper ($r > \lambda$), the incidence of an optical trap originates from a photons transfer of momentum and energy to the object while undergoing a scattering event (reflection, refraction, or diffraction). Since the total momentum and energy of a close system is conserved, the difference in the photon's momentum and energy before and after the scattering event is transferred to the object and can be expressed as a light pressure that is proportional to the intensity of the photons.[11, 12] Since the pressure exerted by a single photon is extremely weak, light must be narrowly focused to a small spot size to maximize the number of photons that interact with the object. For a dielectric particle, the force $F$ that arises from the radiation pressure $P$ is related by $F \propto Pn/c$ , where $n$ is the particle's index of refraction and $c$ is the speed of light.

In the process of narrowly focusing light from a laser source, there arises another force due to the intensity gradients found at the point of highest intensity. Assuming that a dielectric particle consists of many individual dipoles, these dipoles will oscillate in response to the incident electromagnetic field gradients resulting in a Lorentz force toward the direction of highest intensity. This Lorentz or optical force is termed the gradient force and acts primarily in the transverse directions as a restorative force to move the particle back to the center of the beam. The force that arises from the impinging photons' transfer of momentum is aptly named the scattering force which is confined to the axial direction and pushes the particle away from the point of highest intensity.

As Ashkin pointed out early in his research on optical trapping[12], in order to create a three-dimensional optical trap or "tweezer", one must produce a force that counteracts the scattering force. Ashkin's solution to this problem was to tightly focus the laser beam using a high numerical aperture microscope objective. He discovered that the majority of the gradient force resides in the most extreme rays of the focused beam and if the incident angle of these rays is high enough not only will it provide greater transverse stability, but a component of these the rays will exert a force in a direction that opposes the scattering force. The main criterion then for obtaining a stable three-dimensional optical tweezer is that the component of the gradient force along the negative axial direction must cancel out the contribution made by the scattering force.

## 3. SOLID IMMERSION LENS FABRICATION

### 3.1 Fabrication Process

As shown in figure 1, the process of fabricating the polymer SILs employs a high temperature melt and subsequent lift-off technique. To begin with, a metal is thermally evaporated on a quartz substrate to act as a sacrificial layer (A). Polystyrene divinylbenzene microspheres suspended in an alcohol medium are then spin-coated on the substrate at a speed and concentration to maximize the number of microspheres on the substrate yet minimize microsphere aggregation (B). The coated substrate is then heated in order to allow the alcohol to evaporate leaving the microspheres on the substrate's surface (C). The next step involves melting the polymer microspheres by placing the substrate in direct contact with a highly uniform temperature heat source whose temperature is well above the glass transition temperature for a specific amount of time (D). Optimizing the melting time and temperature allows for the transformation of the microsphere into the form of a solid immersion lens. After the correct form of the lens is achieved, the substrate is allowed to cool and the SILs are removed from the substrate by performing a lift-off etch on the metal sacrificial layer (E). The SILs are then washed in a cleaning solution, centrifuged down, and suspended in a predetermined liquid medium (F). Figure 2 displays a picture of a two different 20 μm diameter polymer SILs at the end of the fabrication process.

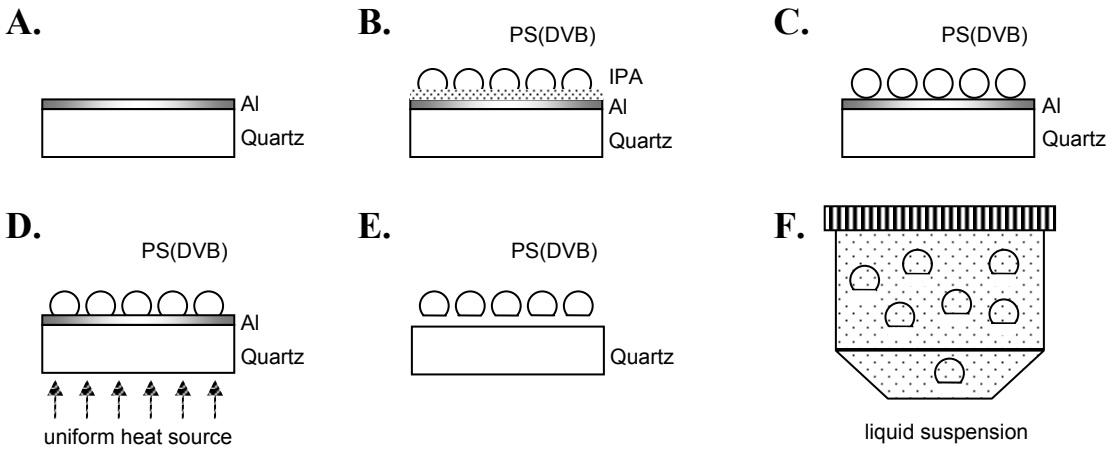


**Figure 1: Fabrication process for the polymer SILs.**

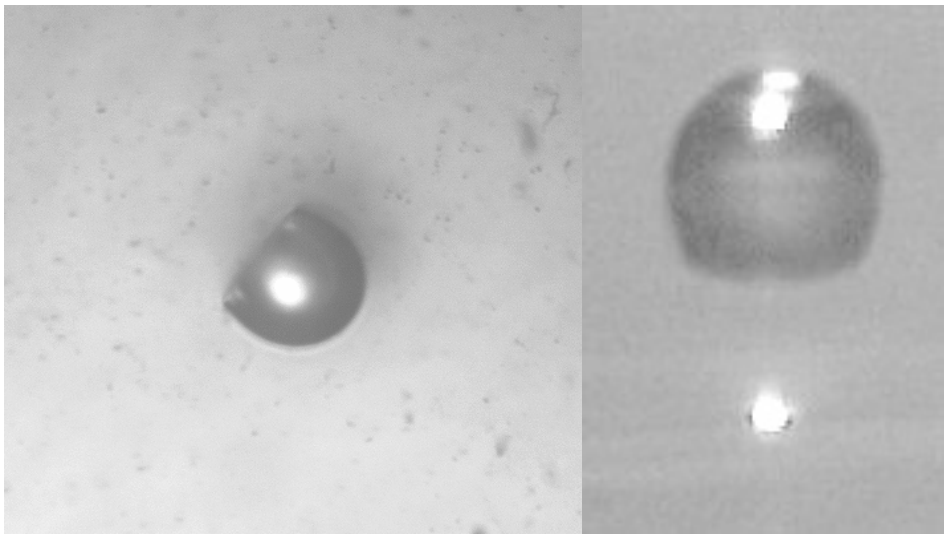

**Figure 2: Post-fabrication photos of two 20μm diameter polystyrene SILs. The picture on the right shows the SIL in direct contact with the glass substrate and focusing the incoherent illumination light into the glass medium.**

### 3.2 SIL Characterization

In order to accurately determine the precise melt time and substrate temperature required to produce the Weierstrass form of the SIL lens we implemented an image processing algorithm to measure the radius of curvature deviation and the thickness of the SIL. The first step of the characterization process involved taking a high resolution digital image of the SIL and importing the raw data from the image into Matlab. Once in Matlab, the edges of the lens are found using the Canny edge detection algorithm provided in the image processing toolbox and the results are displayed in figure 3.

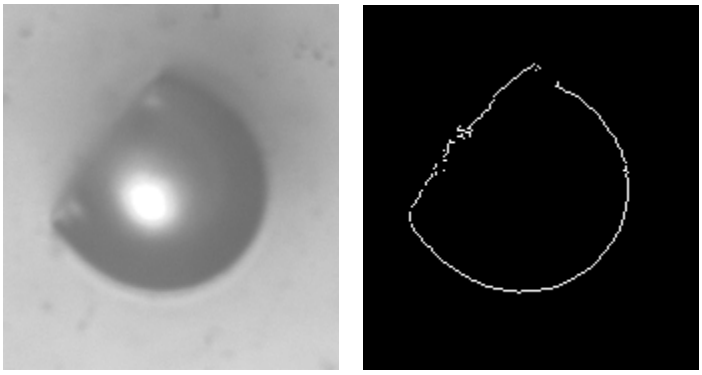

**Figure 3: Results using the Canny edge detection algorithm from Matlab.**

After the edges of the SIL were determined, the center of the upper hemisphere was calculated using the least standard deviation of the distance between pixel and center. The radius of curvature of the lens was then measured by calculating the distance from the center to each point on the hemisphere edge. The thickness of the lens is directly calculated by measuring the distance from center to the top and bottom surface and summing the result. The measurement error associated with this calculation is proportional to the pixel size of the high resolution image. For the 20 μm diameter Weierstrass SIL lens pictured in figure 3, the calculation yielded the following results:

**Measurement Error (Pixel size) = 0.188 μm.**
**Mean Radius = 9.9490 μm**
**Standard deviation = 0.1109**
**Variance = 1.11%.**
**SIL Thickness = 16.48μm.**

Recall that for a Weierstrass SIL, the optimal thickness is given by $r\left(1+1/n\right)$. For a 20 μm diameter polystyrene microsphere with an index of refraction of 1.58, the optimal thickness can be calculated to be **16.329 μm**. In addition the Δz thickness aberration tolerance with this SIL lens using a focusing microscope objective with a NA = 0.9 is approximately equal to **3.9 μm**. Clearly, even with a measurement error of 0.188 μm, our Weierstrass SIL falls well within the acceptable tolerance range. It is also important to note that during the melting process, the radius of curvature of the SIL remains constant, varying only 1.11% across the entire upper hemisphere.

## 4. NEAR-FIELD SOLID IMMERSION MICROSCOPY

### 4.1 Optical System Description

A scanning optical microscope using the microfabricated solid immersion lens is shown in figure 4. This microscope operates both in reflection and transmission imaging modes and the light source is an Ar+ gas laser with a circular $TEM_{00}$ output mode. The laser output first passes through a spatial filter whose output lens expands and collimates the beam to a size that can fill the microscope back aperture. Following the spatial filter the beam passes through a half-wave plate that rotates the polarization of the beam so that it will pass through the polarizing beam splitter. Once past the polarizing beam splitter the polarization is changed from linear to circular using a quarter-wave plate. Next the beam is reflected by a laser line 50-50 beam splitter and coupled into an infinity corrected oil immersion microscope objective with a numerical aperture of 0.9. The microscope objective then focuses the laser beam which is then used to both trap the SIL in the liquid and act as a near-field scanning beam to image the sample through the SIL. The beam transmitted through the sample is then collected with a 0.6 NA microscope objective and focused onto a photodetector. The reflected beam traverses back through the SIL and microscope objective where its polarization is once again changed from circular to linear by the quarter-wave plate but oriented 90 degrees opposite the original state of polarization. On

this pass, the polarizing beam splitter reflects the signal through an iris and onto a second photodetector that records the reflected beams intensity. In addition we have included an incoherent light source and CCD camera to monitor the SILs location and movement. The near-field scanning occurs by fixing the SIL in one position using the laser tweezer and moving the sample relative to the SIL using a 0.1 μm resolution motorized stage.

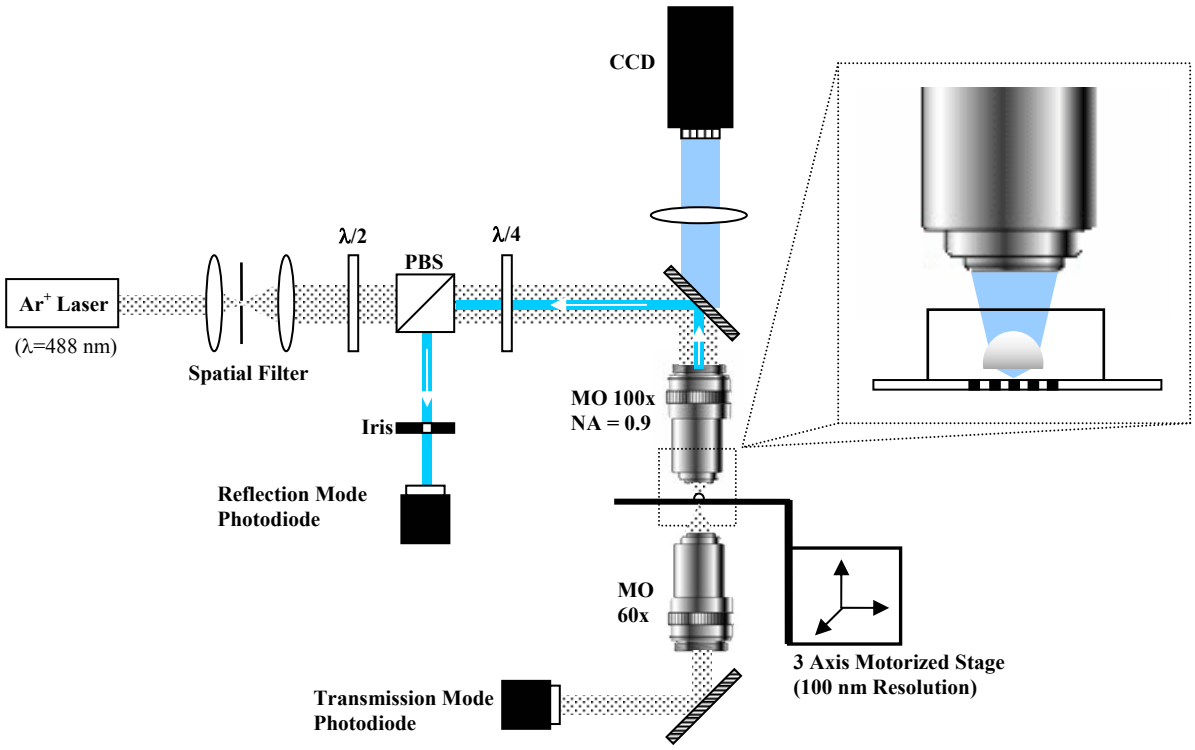


**Figure 4: Solid immersion microscope operating in both reflection and transmission imaging modes.**

### 4.2 Magnification Properties of the SIL

One of the early experiments performed was to test the magnification enhancement of our newly fabricated SIL. The sample used in this case was a chrome grating on a quartz substrate with both a line thickness and grating spacing of one micron. On top of the grating was a 42 μm layer of water covered with a 100 μm glass coverslip. The first step in this process was to perform a reflection mode line scan of a sample using the focused beam from the 0.9 NA microscope objective without the presence of the SIL. Next we performed the same scan except this time introduced a 20 μm diameter Weierstrass SIL, focused the beam a distance *nr* (15.8 μm) beyond the SIL center, and imaged the grating by scanning across the SIL. The resulting pictures obtained from both scans are shown in figure 5. When comparing the two images it is clear to see a definite increase in the magnification of the grating lines when the SIL is placed between the microscope objective and the sample.

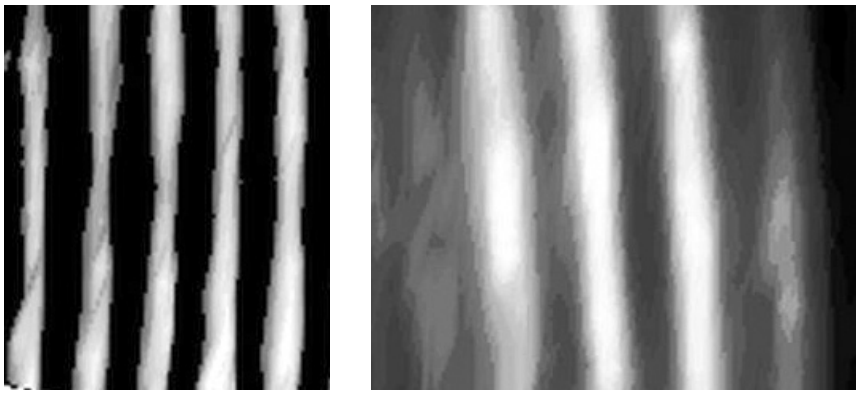

(a) (b)

**Figure 5: Magnification enhancement of the SIL. Part (a) shows the reflection mode line scan of the grating using a 0.9 NA microscope objective without the SIL and (b) with the SIL.**

### 4.3 Reflection Mode Imaging

To demonstrate the imaging capabilities of the solid immersion microscope, reflection mode images of the chrome grating were taken with and without the SIL. In this experiment the size of the SIL that was trapped by the laser tweezer and used to image the grating was 10 μm in diameter. Figure 6 shows the reflected power from a single chrome line in the grating with and without the SIL. Because of the reduced spot size that is produced by the SIL, more light is reflected from the chrome line resulting in a higher power measured at the photodetector.

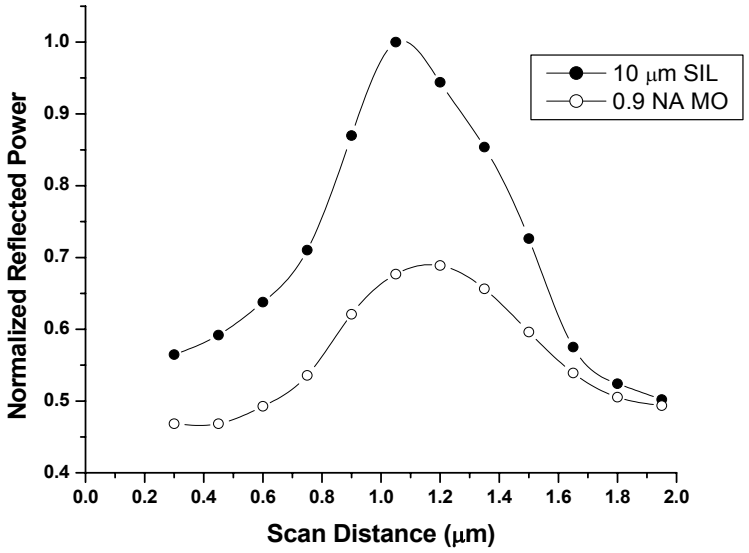


**Figure 6: Reflected power from a single chrome line in the grating vs. scan distance for a 0.9 NA microscope objective with and without the 10μm diameter SIL.**

## 5. SUMMARY

In this paper, we presented a new and novel technique that allows for the integration of a solid immersion microscope into a microfluidic and biological environment. In our system the traditional cantilever mounted SIL is replaced by a laser tweezer controlled, free-floating SIL. We have successfully been able to fabricate polymer Weierstrass SILs using a thermal melting process and have demonstrated extremely high precision in the control of the SIL thickness. Integration of the laser tweezer and polymer SIL into a solid immersion microscope has proven to be successful and preliminary experiments involving the magnification properties of the SIL and reflection mode imaging using the SIL show a definite improvement in resolution when compared to results obtained from the microscope objective without the SIL.

## 6. ACKNOWLEDGEMENTS

We would like to thank the Defense Advance Research Project Administration (DARPA) via the CHIPS Opto-Center and the University of California, San Diego for supporting this research.

## 7. REFERENCES

1. R. Juskaitis, "Characterizing High Numerical Aperture Microscope Objective Lenses," in *Optical imaging and microscopy : techniques and advanced systems*, F.-J. Kao and P. Torok, Eds., pp. 21-43, Springer-Verlag, New York, 2003.
2. M. Ohtsu, "Near-Field Optical Microscopy and Application to Nanophotonics," in *Optical imaging and microscopy : techniques and advanced systems*, F.-J. Kao and P. Torok, Eds., pp. 339-355, Springer-Verlag, New York, 2003.
3. G. S. Kino, "Fields associated with the solid immersion lens," *Far- and Near-Field Optics: Physics and Information Processing*, **3467**, pp. 128-37, SPIE-Int. Soc. Opt. Eng. Proceedings of Spie - the International Society for Optical Engineering, San Diego, CA, USA, 1998.
4. G. S. Kino, "Applications and theory of the solid immersion lens," *Optical Pulse and Beam Propagation*, **3609**, pp. 56-66, SPIE-Int. Soc. Opt. Eng. Proceedings of Spie - the International Society for Optical Engineering, San Jose, CA, USA, 1999.
5. B. D. Terris, H. J. Mamin, D. Rugar, W. R. Studenmund, and G. S. Kino, "Near-field optical data storage using a solid immersion lens," *Applied Physics Letters*, vol. **65**, pp. 388-90, 1994.
6. Y. Youngjoo, B. Jong Uk, C. Il-Joo, Y. Euisik, M. Su-Dong, and K. Shinill, "Micro solid immersion lens fabricated by micro-molding for near-field optical data storage," *2000 IEEE/LEOS International Conference on Optical MEMS* pp. 91-2, IEEE, Piscataway, NJ, USA., Kauai, HI, USA, 2000.
7. F. Guo, T. E. Schlesinger, and D. D. Stancil, "Optical field study of near-field optical recording with a solid immersion lens," *Applied Optics*, vol. **39**, pp. 324-32, 2000.
8. M. Born and E. Wolf, *Principles of optics : electromagnetic theory of propagation, interference and diffraction of light*, 7th (expanded) ed., Cambridge University Press, Cambridge; New York, 1999.
9. W. Qiang, L. P. Ghislain, and V. B. Elings, "Imaging with solid immersion lenses, spatial resolution, and applications," *Proceedings of the IEEE*, vol. **88**, pp. 1491-8, 2000.
10. K. B. Crozier, D. A. Fletcher, G. S. Kino, and C. F. Quate, "Micromachined silicon nitride solid immersion lens," *Journal of Microelectromechanical Systems*, vol. **11**, pp. 470-8, 2002.
11. A. Rohrbach, J. Huisken, and E. H. K. Stelzer, "Optical Trapping of Small Particles," in *Optical imaging and microscopy : techniques and advanced systems*, F.-J. Kao and P. Torok, Eds., pp. 357-386, Springer-Verlag, New York, 2003.
12. A. Ashkin, J. M. Dziedzic, J. E. Bjorkholm, and S. Chu, "Observation of a single-beam gradient force optical trap for dielectric particles," *Optics Letters*, vol. **11**, pp. 288-90, 1986.